Low Temperature Physics

Elastic, magnetoelastic, magnetopiezoelectric, and magnetodielectric characteristics of $HoAl_3(BO_3)_4$

Cite as: Low Temp. Phys. **46**, 923 (2020); https://doi.org/10.1063/10.0001715
Submitted: 22 July 2020 . Published Online: 30 September 2020

I. V. Bilych, M. P. Kolodyazhnaya, K. R. Zhekov, G. A. Zvyagina, V. D. Fil, and I. A. Gudim

Low Temperature Physics ARTICLE scitation.org/journal/ltp

Elastic, magnetoelastic, magnetopiezoelectric, and magnetodielectric characteristics of $HoAl_3(BO_3)_4$

Cite as: Fiz. Nizk. Temp. **46**, 1092–1101 (September 2020); doi: 10.1063/10.0001715
Submitted: 22 July 2020

I. V. Bilych,[1] M. P. Kolodyazhnaya,[1] K. R. Zhekov,[1] G. A. Zvyagina,[1] V. D. Fil,[1,a)] and I. A. Gudim[2]

AFFILIATIONS

[1]B. Verkin Institute of Low Temperature Physics and Engineering, National Academy of Sciences of Ukraine, Kharkov 61103, Ukraine
[2]Kirensky Institute of Physics, Siberian Branch of the Russian Academy of Sciences, Krasnoyarsk 660036, Russia

[a)]**Author to whom correspondence should be addressed:** fil@ilt.kharkov.ua

ABSTRACT

The main elastic moduli and piezoelectric modulus have been measured in holmium alumoborate single crystals. The renormalization of the permittivity, piezoresponse, and sound velocities, driven by the nematic-like paramagnetic phase in the sample, is considered. A significant variability of the results is detected, which is caused, presumably, by the fact that, under the action of external fields, the motion trajectory of the nematic-like phase's director depends on random defects of thermoelastic origin. It is shown that above 5 K, the temperature dependences of the studied parameters are well-described using holmium ion's known ground multiplet spectrum, formed by the interaction with the crystal field. Changes in the C_{44}-mode velocity in the sub-Kelvin temperature range are measured.

INTRODUCTION

The $HoAl_3(BO_3)_4$ compound has received considerable attention due to its remarkable magnetoelectric characteristics. According to literature data,[1] at low temperatures (5 K) and in a field of ~9 T, the magnetic field-stimulated electric polarization of some geometric configurations reaches record values of ~5000 μC/m^2. Interest in studying magnetoelectric effects is driven by the alleged possibilities of using them in non-dissipative systems for recording and reading information. The most promising objects in this regard are the so-called ferroelectromagnets (or multiferroics), which are substances that combine antiferromagnetic and ferroelectric properties. Their magnetoelectric response is caused by the action of their own exchange field, and an experimental external field is needed only for monodomainization. Holmium alumoborate is paramagnetic up to sub-Kelvin temperatures, with no signs of observable magnetic ordering, and therefore the magnetoelectric response (electric polarization) appears only in an external field. Nevertheless, the study of $HoAl_3(BO_3)_4$ single crystals is of considerable interest, since it allows for a deeper understanding of the physical mechanisms responsible for the appearance of electric polarization under the action of a magnetic field.

Below is a summary of the information on the range of topics discussed in the article, available to date.

1. The characteristics of polarization related to its temperature and magnetic field behavior, which manifests when the latter is applied in the basal plane, were studied in detail.[1–5] Qualitatively, the results presented in these studies were similar, however, there was significant scatter of quantitative data: the polarizations measured under identical conditions and on samples of common origin differed by several factors. The authors of Ref. 4 believe that this behavior is explained by different ratios of enantiomorphic phases. As determined in this article, prehistory is also significant, because the results obtained for the same sample, but in different measurement cycles, may vary. This observation is illustrated below by results from the same type of experiments, performed both with a three-month interval (Figs. 1 and 3–5) and on the same day, but separated by heating–cooling cycles (Fig. 7).
2. In Refs. 2 and 4, data on the intensity of magnetoelastic interaction were obtained by studying magnetostrictive effects. The magnetostrictive deformations' order of magnitude turned out to be almost gigantic (~10^{-4} at 6 T).
3. The magnetodielectric effect was studied in Refs. 3 and 4. At liquid helium temperatures, the permittivity of the basal plane underwent a field-dependent change of about several percent.
4. The parameters of the crystal field and energy structure of the Ho^{3+} ion $^5I_8$ ground term ($S = 2$, $L = 6$, $J = 8$, $g_J = 5/4$), and

calculations of the magnetic susceptibility and magnetostriction based on these parameters, are discussed in Refs. 1, 6, and 7. A somewhat different position for the ground term energy levels is obtained while maintaining the same systematics, when studying the optical spectra of yttrium aluminum borate diluted with holmium.[8]

To summarize the presented information, we can confirm that there is a complete absence of experimental data on the magnitude and behavior of elastic and piezoelectric moduli. There is only one article devoted to the theoretical calculation of these characteristics, within the framework of the density functional method.[5] This publication partially addresses this gap. In addition to determining the values of the required moduli, considerable attention is paid to the study of the temperature and magnetic-field dependences of the permittivity, piezomoduli, and sound velocity, including anisotropy with respect to the direction of the magnetic field.

ELASTICITY MODULI AND PIEZOMODULUS

The research samples were cut from a single-crystal ingot, grown according to the technique described in Ref. 9 and oriented by the X-ray method. Orientation accuracy ~1°, typical sample dimensions ~3 mm. The absolute velocities of sound s were measured using the setup described in Ref. 10, at frequencies of ~55 MHz and liquid nitrogen temperature. Measurement accuracy ~0.5%. The results are shown in Table I.

An algorithm for determining the elastic moduli and piezomodulus for the specific trigonal crystallographic group $R32$ is given in Ref. 11. The X-ray density $\rho = 4.46$ g/cm^3 and permittivity $\varepsilon = 26$ are used in the calculations.[4] The results are presented in Table II.

The error of determining the numerical values (with the exception of the noted cases) is about 1%. Modulus C_{14} is defined by expression: $C_{14} = C_{44}\sqrt{\left[1-\left(\frac{s_{yz}}{s_{zy}}\right)^2\right]\left[\left(\frac{s_{yy}}{s_{zy}}\right)^2-1\right]}$, and therefore, the accuracy of its definition is low. We emphasize that the reliable execution of the required condition $s_{yz}/s_{zy}<1$ in the experiments confirms the claimed accuracy of the measurement procedure. The magnitude of the piezomodulus is found from the ratio $e_{11}^2 = \frac{(s_{xx}^2-s_{yy}^2+s_{zy}^2-s_{yz}^2)\varepsilon\rho}{4\pi}$, and its accuracy is determined by the longitudinal mode velocity ratio, and the errors therein. The sought-after piezomodulus is also evaluated by comparing the potentials excited by the same deformation in α-quartz and the studied sample. Taking into account the geometric factors, an almost identical result is obtained $e_{11} \approx 1.6 \pm 0.2$. In these measurements, the scatter of estimates is caused by the irreproducibility of acoustic binder characteristics. The calculation in Ref. 5 is in qualitatively good agreement with the experiment that confirms the increased rigidity of the crystals with respect to the tensile-compression in the basal plane.

TABLE I. The velocities of sound in $HoAl_3(BO_3)_4$. In the mode indication, the first subscript corresponds to the direction in which the oscillations propagate, and the second is the orientation of the displacement at the excitation interface.

Mode	u_{zz}	u_{zy}	u_{xx}	u_{yy}	u_{yz}	u_{yx}
s (10^5 cm/s)	7.46	4.03	9.70	9.61	3.95	4.88

TABLE II. Elastic moduli (GPa) and piezomodulus (C/m^2) in $HoAl_3(BO_3)_4$.

Modulus	C_{11}	C_{33}	C_{44}	C_{12}	C_{14}	e_{11}
Our data	409	248	72	217	31 ± 5	1.56 ± 0.2
Ref. 5 calculation	395	173	64	131	10	1.75

MAGNETOCAPACITY AND MAGNETOPIEZOELECTRIC EFFECT

The terms magnetocapacity and magnetopiezoelectric effect mean that the changes in the permittivity ε and piezomodulus e are correlated with how the state of the magnetic subsystem evolves. For example, in ferroborates that are isostructural to the compound under study, the effective values of ε and e increase considerably with antiferromagnetic ordering.[12–14] The imposition of an external magnetic field also leads to changes in the dielectric and piezoelectric responses. The common reason for the existence of such correlations is the so-called rotational susceptibility. If the ion carrying the magnetic moment is not in the S-state, then the electron cloud creating the orbital momentum is a rather rigid aspherical "spindle" formation, the orientation of which is determined by the crystal field. If the anisotropy of the latter is not too large, the spindle rotates under the action of external fields (electric, elastic, and magnetic), thus deforming the lattice. As a result, polarization appears, ε and e change, as does the lattice rigidity. In addition, a change in the symmetry, together with magnetic ordering, leads to the appearance of new, previously forbidden components of the piezomodulus tensor,[15] and allows for the piezoelectric effect to exist in a crystallographically centrosymmetric structure.[16]

Holmium alumoborate is paramagnetic at all temperatures studied, however, the interaction of the rare-earth ion and a crystal field leads to the formation of an anisotropic paramagnetic state in the low temperature limit. According to magnetic measurements,[1,2] the susceptibility, being practically isotropic at high temperatures, acquires an Ising-like character in the helium region. In other words, the magnetic moment distribution acquires a nematic motif, which can be characterized by a director oriented along the trigonal axis. It is also impossible to exclude the establishment of a cholesteric phase, since in the absence of an inversion center, the nematic phase is unstable with respect to the formation of helicoidal structures.[17]

Below are the results of measuring the relative temperature and magnetic field changes of the permittivity and piezomodulus, when the electric field or longitudinal deformation is oriented along the main directions in the basal plane of $HoAl_3(BO_3)_4$. The equipment used is described in Ref. 10. The measurement technique is described in detail in Ref. 12. The accepted measurement method makes it possible to estimate the piezomodulus according to the magnitude of the electric potential excited by the elastic deformation in the interface layer.

Figure 1 shows the results of measuring the evolution of permittivity in the absence of a magnetic field. The permittivity behavior is observed as having significant anisotropy: the component ε_{zz} does not depend on temperature, within error. Qualitatively, this effect has a simple interpretation: the measurement field, parallel to the director, does not change the symmetry of the problem, and the electron cloud, regardless of the degree of its anisotropy, retains its orientation. The rotational susceptibility appears in the transverse field deflecting the director, and increases with decreasing temperature and the corresponding development of asphericity. Also, note the variability in the scale of the temperature changes for the transverse components of permittivity, obtained for the same sample during different measurement cycles, illustrated by the example of the ε_{xx} parameter (curves 1 and 2). No action, such as heat treatment, was taken with the sample between these experiments. We believe that this variability is associated with the irreproducibility of the distribution of the thermoelastic defects that affect the rotational susceptibility and arise during sample cooling. The behavior of ε_{yy} is quantitatively and qualitatively similar to ε_{xx}. Due to the observed variability, it is impossible to draw conclusions about any manifestations of permittivity anisotropy in the basal plane during these experiments.

Figure 2 shows the relative change in the piezomoduli; e_{22} is shown together with the e_{11} component. The $HoAl_3(BO_3)_4$ piezoresponse to deformation u_{yy} is about an order of magnitude less than the response to deformation u_{xx} (note that Fig. 2 shows relative changes). Nevertheless, it is reliably observed, even though in a crystal with the space group $R32$ the existence of a nonzero e_{22} component is incompatible with C_2 symmetry. A similar effect has been previously observed in the paraphase of the $SmFe_3(BO_3)_4$ ferroborate,[15] where it was associated with the surface piezoelectric effect. It exists due to the removal of symmetry constraints (C_2 axis) in the surface interface layer.[15] The manifestation of the response could also be associated with the structural rearrangement of the interface layer that occurs due to the thermoelastic stresses, which arise during the solidification of the acoustic binder (~120 K). This effect, previously observed in $LiCoPO_4$,[18] appears in a jump-like manner and has a hysteresis nature. To check for this possibility, we measured e_{22} at higher temperatures (in Fig. 2, the acoustic binder's contribution to the change in the recorded amplitude is subtracted). The absence of any features, such as jumps, in the acoustic binder softening region makes it possible to exclude this assumption.

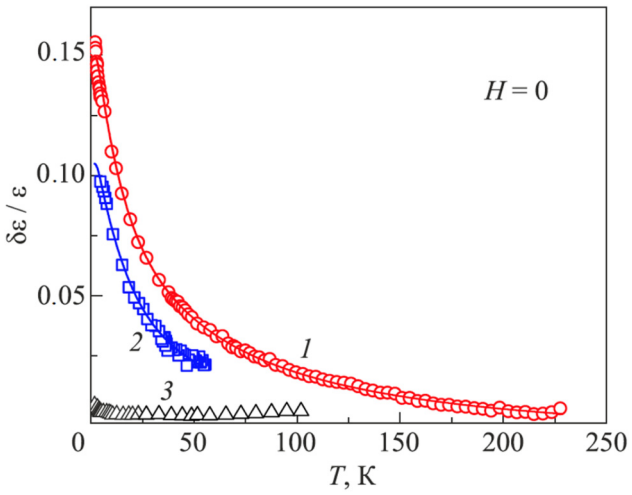

FIG. 1. Relative permittivity as a function of temperature, in the absence of a magnetic field. (1) ε_{xx} (measurements on 10.17.2019): (2) ε_{xx} (measurements on 04.05.2019); (3) ε_{zz}. Solid lines are calculated curves obtained using Eq. (3) with parameters: $a_1 = 0.3$, $a_5 = -0.2523$, $a_7 = -0.1699$ (curve 1) and $a_1 = 0.209$, $a_5 = -0.245$ (curve 2).

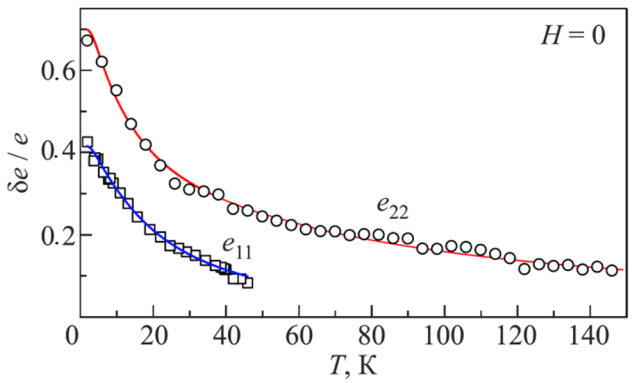

FIG. 2. Relative piezomoduli as a function of temperature, in the absence of a magnetic field. Symbols represent the experiment, solid lines show the calculated curves obtained using Eq. (3) with parameters: e_{22}: $b_1 = 1.4, b_5 = -0.528$, $b_7 = -0.848$ and for e_{11}: $b_1 = 0.825, b_5 = -0.918$.

The contributions of the magnetoelectric and magnetoelastic interactions to the free energy F_{meu}, for fields oriented in the basal plane along the main crystallographic directions, which are relevant for our consideration, can be represented as[19]

$$F_{meu} = E_x\left(A_{21}\langle\Omega_2^1\rangle + A_{22}\langle O_2^2\rangle\right) + E_y\left(A_{21}\langle O_2^1\rangle - A_{22}\langle\Omega_2^2\rangle\right) + (u_{xx} - u_{yy})\left(B_{21}\langle\Omega_2^1\rangle + B_{22}\langle O_2^2\rangle\right) + \sum_{n=4,6}\langle\Delta_n\rangle. \quad (1)$$

Here, A_{im}, B_{im} are the phenomenological coefficients of the magnetoelectric and magnetoelastic interactions, $\langle\Omega_2^m, O_2^m\rangle$ are the thermal averages of equivalent tensor operators calculated with respect to the energy spectrum and wave functions of the ground $^5I_8$ multiplet of the Ho^{3+} ion. The last term in Eq. (1) symbolizes the contributions of higher order multipole moments, also accompanied by their own phenomenological coefficients. In fact, tensor operators are permitted combinations of an ion's total magnetic moment components, invariant with respect to the crystal symmetry group, taking into account the time inversion. Specific expressions for the first multipole moments applied to a trigonal crystal can be found in Ref. 19.

The effective permittivity and piezomodulus are determined by expressions[20]

$$\varepsilon_{ii}^{\text{eff}}(T) = \varepsilon_{ii}^{0} - 4\pi\frac{\partial^2 F_{meu}}{\partial E_i^2}, \quad e_{ii}^{\text{eff}}(T) = e_{ii}^{0}\frac{\partial^2 F_{meu}}{\partial E_i \partial u_{ii}}, \tag{2}$$

where the superscript 0 denotes the corresponding parameters, without taking magnetic contributions into account. Since F_{meu} contains quite a lot of coefficients which fitted by comparision to the experiment, one can skip calculating the matrix elements of the equivalent operators included in (1), and immediately transition to a phenomenological representation of the relative changes in the discussed characteristics, within the framework of perturbation theory:

$$\frac{\delta\varepsilon_{xx}(T)}{\varepsilon_{xx}^{0}} = \frac{\sum_i a_i \exp(-E_i/T)}{Z}, \qquad \frac{\delta e_{11}(T)}{e_{11}^{0}} = \frac{\sum_i b_i \exp(-E_i/T)}{Z}. \tag{3}$$

In Eq. (3), E_i are the energy levels of the Ho^{3+} ion ground $^5I_8$ multiplet, $Z = \sum_i \exp\left(-\frac{E_i}{T}\right)$ is the partition function, a_i,b_i are phenomenological parameters representing the "acceleration" with which the i-level moves along the energy scale, due to the influence of external fields. In the case of a doublet, this refers to the behavior of its center of gravity.

In a trigonal crystal field, the energy spectrum of the Ho^{3+} ion ground $^5I_8$ multiplet is represented by 11 lines, six of which are doubly degenerate. The lower levels relevant to the problem under consideration, found by approximating the temperature dependence of the $HoAl_3(BO_3)_4$ magnetic susceptibility,[7] are given in Table III. It also shows the values of E_i obtained by analyzing the optical spectra of yttrium aluminum borate diluted with holmium.[8]

To describe the temperature changes below 40 K, it is sufficient to restrict ourselves to the first six levels from Ref. 7. When performing calculations, it is convenient to account for levels 5 and 6 as a quasi-doublet, separated from the origin by 41 K. The procedure for fitting the phenomenological coefficients is quite simple. It is obvious that for the lowest doublet $i = 1, 2$, the corresponding coefficients are practically determined by the values of the measured responses in the low temperature limit (Due to the fact that the doublet is taken into account twice, the corresponding coefficient in Eq. (3) is twice the recorded response). The only parameter that can be freely changed is the position of the described dependence with respect to the unperturbed level, since it cannot be known precisely due to the limited measurement temperature range.

TABLE III. Structure of the lowest energy levels of the Ho^{3+} ion ground $^5I_8$ multiplet in $HoAl_3(BO_3)_4$.

i	1, 2	3, 4	5	6	7	8, 9
E_i, K[7]	0	12	36	47	162	226
E_i, K[8]	0	18	20	50	180	200

The most interesting result of the approximation procedure is that for the dependences shown in Figs. 1 and 2, the contribution of the doublet with $i = 3, 4$ in the numerator of Eq. (3) turns out to be negligible. It can always be neglected, leaving this contribution as the partition function. Since this feature turns out to be true for practically all the studied dependences, its existence is hardly accidental and seems to indicate that neither the electric field, nor the longitudinal deformation, acting in the basal plane, affect the position of this doublet's center of gravity.

As such, in order to describe the temperature behavior of the studied dependences below 40 K by the numerators of Eq. (3), it is enough to restrict ourselves to the constant term ($i = 1, 2$) and the exponential contribution from the quasi-doublet ($i = 5, 6$). For the temperature range up to 200 K, the contribution from the nearest singlet ($i = 7$) is added. The full set of levels presented in Table III is used when calculating the partition function. To avoid discrepancies, let us emphasize that all calculations are carried out by taking into account the degree of degeneracy of the levels, i.e., each doublet is counted twice. An illustration of the "quality" of the approximation is shown in the presented figures. Significant deviations appear only below 5 K, and they seem to be associated with ground doublet splitting due to hyperfine interaction and the Jahn–Teller effect.[8]

We implemented a trial approximation procedure using the system of levels from Ref. 8 (bottom row of Table III). The quality of the approximation with slightly different coefficients turned out to be practically the same, however, it was found that the contributions of not only the doublet with $i = 3, 4$, but also the singlet with $i = 5$ are negligibly small, which seems physically unjustified. It appears that the spectrum from Ref. 7 is closer to reality, as applied to $HoAl_3(BO_3)_4$.

We will discuss the possible reasons behind the variability of the discussed curves. Let us supplement Eq. (1) with an important term related to the component of the crystal field Hamiltonian $F_{CF} \sim \alpha\langle O_2^0\rangle (\alpha < 0)$. At helium temperatures, the system is in the ground state, and the operators in Eq. (1) can be replaced with mean values. Let us rewrite Eq. (1) in angular coordinates that determine the orientation of the resultant moment. Since F_{CF} changes quadratically near the equilibrium polar angle $\theta = 0, \pi$ (these states are equivalent due to the degeneracy of our nematic-like phase with respect to the director direction), and the first-order multipole moments are linear, then when an external transverse field is applied, it is always possible to establish a state with a low energy at certain angular variables, i.e., the latter are functions of the external field.

Having performed calculations (2), and assuming that the value of the polar angle is equal to the equilibrium value in the final expressions, we see that changes in the discussed parameters are determined only by the terms in Eq. (1) with $m = 1$. For changes in ε and e, we obtain the relations:

$$\frac{\delta\varepsilon_{xx}}{\varepsilon_{xx}^{0}} = \frac{16\pi}{\varepsilon_{xx}^{0}}\frac{A_{21}^2\sin^2\varphi}{\partial^2 F/\partial\Theta^2}, \quad \frac{\delta e_{11}}{e_{xx}^{0}} = \frac{4A_{21}B_{21}}{e_{11}^{0}}\frac{\sin^2\varphi}{\partial^2 F/\partial\Theta^2}. \tag{4}$$

In Eq. (4), φ is the azimuthal angle measured from the axis $x||C_2$. In fact, with an average value of θ = 0, π, the φ coordinate determines the oscillation trajectory of the magnetic moment associated with the ion, when a transverse alternating field is applied. In a homogeneous state, when measured in the field $\mathbf{E}||x$ or elastic deformation u_{xx}, it follows from the stationarity conditions that this trajectory lies in the yz plane (φ = π/2 or 3π/2), and that the response (4) is at a maximum. However, the cholestericity, as well as the appearance of random thermoelastic-stress induced u_{iz} deformations in the sample, will lead to local displacements of the director from the C_3 axis, due to the magnetoelastic interaction. The trajectory of its movement will also change under the action of an external force, i.e., there will be variability in response (4), which is what seems to be observed in experiments.

Let us also refer to the piezoelectric response to deformation u_{yy}. Carrying out calculations similar to Eq. (4), we obtain the relation

$$e_{22} = 4A_{21}B_{21}\frac{\sin 2\varphi}{\partial^2 F/\partial\Theta^2}. \quad (5)$$

In a homogeneous state, under the action of u_{yy} deformation, the parameter φ assumes the same value as under deformation u_{xx}, and the response (5) is zeroed. Consequently, the existence of the e_{22} piezoresponse is associated either with the surface piezoelectric effect, or with the violation of C_2 symmetry in the bulk, near the defects. Nevertheless, the temperature dependence of the response is well approximated by relations such as Eq. (3) with a negligible contribution of the doublet with $i = 3, 4$ (Fig. 2).

The magnetic field dependences also show significant variability. Figure 3 displays the measurement results of the magnetodielectric response for three selected directions of the field in the basal plane φ = 0, π/4, π/2, obtained in two experiments (03.05.2019 and 12.03.2018). The sample was kept at room temperature between these experiments. Figure 4 shows the orientation dependences of the dielectric response in a fixed field, obtained during the same cooling cycles. Similar results for the piezoresponse are shown in Fig. 5. In all cases, the results of experiments performed on

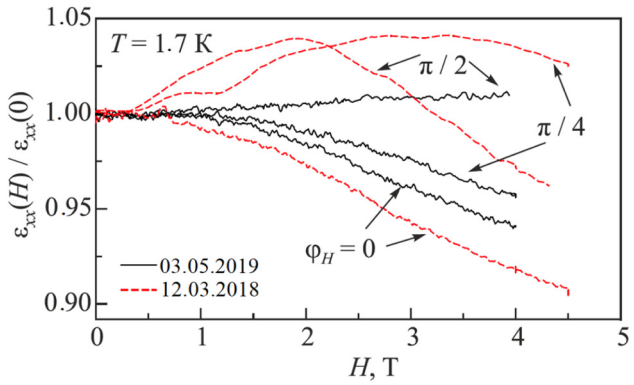

FIG. 3. Magnetic field dependences ε_{xx} for different directions of the magnetic field H in the basal plane. Solid lines show measurements dated 03.05.2019, dashed lines show measurements dated 12.03.2018.

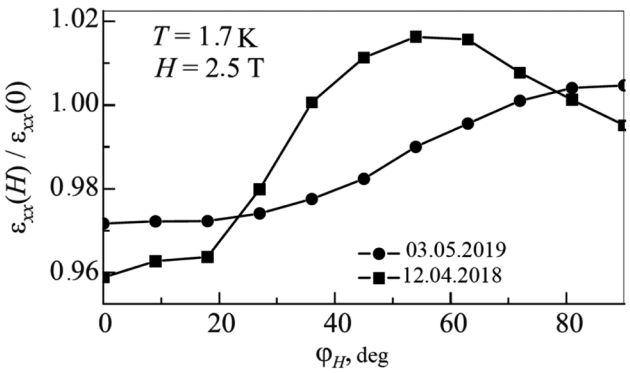

FIG. 4. Dependence of ε_{xx} on the orientation of the magnetic field H in the basal plane. (●) show measurements dated 03.05.2019, (■) show measurements dated 12.04.2018.

different days are irreproducible, which is especially significant when the magnetic field deviates from the C_2 axis.

The interpretation of such dependences is also based on Eqs. (1) and (2). In this case, perturbation theory methods should be used to separate the terms associated with the Zeeman variations of the magnetic ion spectrum, in the thermodynamic potential. In the low temperature limit ($T \ll E_{2,3}$), taking into account the symmetry constraints, the contribution of the magnetoelectric interaction to the thermodynamic potential, for an electric field directed along $x||C_2$, assumes the form[21]

$$F_{me} = E_x[a_{||}(m_x h_x - m_y h_y) + a_{\perp} m_z h_y]. \quad (6)$$

Here m_i, h_i are the direction cosines of the magnetic moment associated with the ion and the external magnetic field, respectively. It is assumed that the latter lies in the basal plane at an angle φ_H to

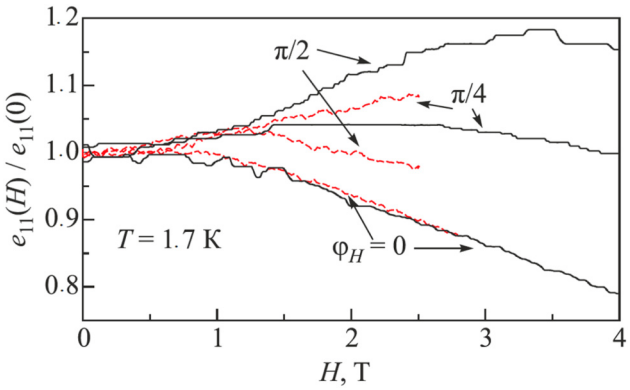

FIG. 5. Magnetic field dependences of the piezomodulus e_{11} for different directions of the magnetic field H in the basal plane φ = 0, π/4, π/2. Solid lines show measurements dated 03.29.2019, dashed lines show measurements dated 12.10.2018.

the x axis, and is enough to overcome the crystallographic anisotropy, i.e., the director of the nematic-like phase is oriented approximately parallel to the field. The dimensional phenomenological coefficients $a_{||,\perp}$ characterize the rotational susceptibilities in the basal plane and perpendicular to it. Transitioning to the angular variables, we get:

$$F_{me} = E_x(a_{||}cos(\varphi + \varphi_H)sin\vartheta + a_\perp \sin\varphi_H cos\vartheta). \quad (7)$$

Calculating the corresponding derivatives in Eq. (2), taking into account the dependence of θ and φ on the external electric field, and setting $\varphi = \varphi_H$ and $\vartheta = \pi/2$ in the final expressions, we confirm that, in this case, it is important to account for terms with $m = 1$, and with $m = 2$ in Eq. (1). For changes in ε, we obtain

$$\delta\varepsilon_{xx}(H) = \varepsilon_{xx}(H) - \varepsilon_{xx}(0) = \frac{4\pi a_{||}^2 \sin^2 2\varphi_H}{\partial^2 F/\partial\varphi^2} + \frac{4\pi a_\perp^2 \sin^2\varphi_H}{\partial^2 F/\partial\theta^2}. \quad (8)$$

The change in the piezomodulus is described by an expression similar to (8), wherein $4\pi a_i^2$ is replaced by $a_i b_i$. Note that for a fixed value of the magnetic field, Eq. (8) represents a dependence that is asymmetric with respect to the rotation of H from the x-axis to the y-axis. In the previously studied easy-plane ferroborates,[12,13] to which Eq. (8) is equally applicable, an almost symmetric change in the permittivity and piezomodulus is observed when H is rotated from the x-axis to the y-axis. This was caused by increased rigidity with respect to the magnetic vector deviation from the basal plane, and the practical absence of any contribution from the last term in Eq. (8) to the measured characteristics. The situation is entirely different for $HoAl_3(BO_3)_4$, since its orientational dependences are noticeably asymmetric (Figs. 3–5). We believe that this behavior is caused by an increased rotational susceptibility relative to the deviation of magnetic vectors from the basal plane. The variability of the results is caused by the fact that this susceptibility largely depends on the degree of defectiveness of the crystal, which is determined by the contribution of poorly controllable thermoelastic stresses.

SOUND VELOCITY

The elastic moduli C_{ik}, and the corresponding elastic wave velocities, are also renormalized to rotational susceptibility. The elastic moduli are defined as the second derivative of the thermodynamic potential with respect to the corresponding deformation. In addition to elastic energy, piezoelectric interaction should also be included in the consideration. Taking the latter into account when observing the electroneutrality requirement leads to a hardening of the lattice $\delta C = 4\pi e^2/\varepsilon$.[20] When the magnetoelastic and magnetoelectric interactions are included in the consideration, the formulation of this expression is conserved, however, the effective values of ε and e (2), (3) considered above should be understood as the piezomodulus and permittivity.[12] Recall, also, that renormalization to rotational susceptibility is possible only when the external field (in this case, elastic deformation) can change the orientation of the director.

Singling out the contribution to the velocity of the u_{ik} mode that appears in response to the developing of the nematic-like paramagnetic phase, we obtain the expression

$$\frac{\delta s}{s} = \frac{1}{2\rho s^2}\left[\frac{4\pi(e^{\text{eff}})^2}{\varepsilon^{\text{eff}}} - \frac{4\pi(e^0)^2}{\varepsilon^0} + \frac{\partial^2 F_{mu}}{\partial u_{ik}^2}\right]. \quad (9)$$

Transitioning, as before, to the low temperature limit and angular coordinates, it is easy to verify that, in the case of longitudinal sound ($i = k$), Eq. (9) gives a nonzero solution in the ground state ($\theta \approx 0, \pi$) only for $i = x, y$. The last term in Eq. (9) assumes the form

$$\frac{\partial^2 F_{mu}}{\partial u_{ii}^2} = -\frac{4B_{21}^2 \sin^2\varphi}{\partial^2 F/\partial\Theta^2}. \quad (10)$$

The meaning of the angular coordinate φ is the same when the polar angle is close to the mean value. This contribution to the renormalization of velocity is always negative. The two remaining terms are defined by the piezoelectric interaction; their interference is positive, although the general result of Eq. (9) is always negative. The piezoelectric contribution is noticeable, comparable with the magnetoelastic contribution in terms of absolute values, and compensates for it to a large extent, only under deformation u_{xx}. Since e_{22}^{eff} is at least an order of magnitude less than e_{11}^{eff}, it is expected that the change in the velocity of the u_{yy}-mode should be noticeably larger.

Figure 6 shows the longitudinal sound velocity as a function of temperature, for the wave vector directions along the main crystallographic directions. As expected, the u_{zz}-mode does not go through significant softening. Despite the fact that the results of these experiments also show variability, on average, the scale of the changes due to deformation u_{xx} is two to three times less than under u_{yy}, which is consistent with the above conclusion.

The temperature evolution of the discussed elastic characteristics (9) can also be reduced to expressions that resemble Eq. (3), but with their own phenomenological coefficients, c_i. Figure 6 shows the approximation curves together with the experimental data. The main result of these calculations is consistent with the

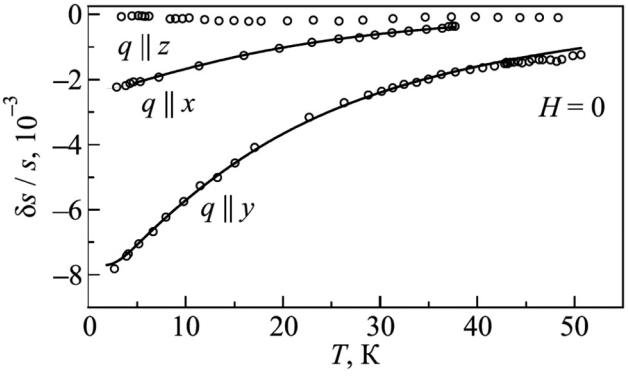

FIG. 6. Relative changes of the longitudinal velocity of sound as a function of temperature, in the absence of a magnetic field. (○) show the experiment, solid lines show the calculated curves obtained using an expression similar to (3), with phenomenological coefficients c_i: for $q \parallel x$, $c_1 = -0.0046$, $c_5 = 0.0088$; for $q \parallel y$, $c_1 = -0.0154$, $c_5 = 0.024$.

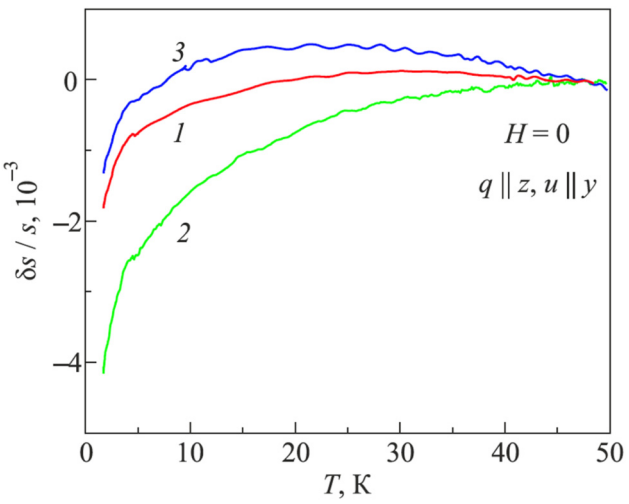

FIG. 7. Variability of the relative changes in the velocity of the C_{44}-mode, in the absence of a magnetic field. 1, 2, 3 is a sequence of measurements performed on the same day. Sample No. 1.

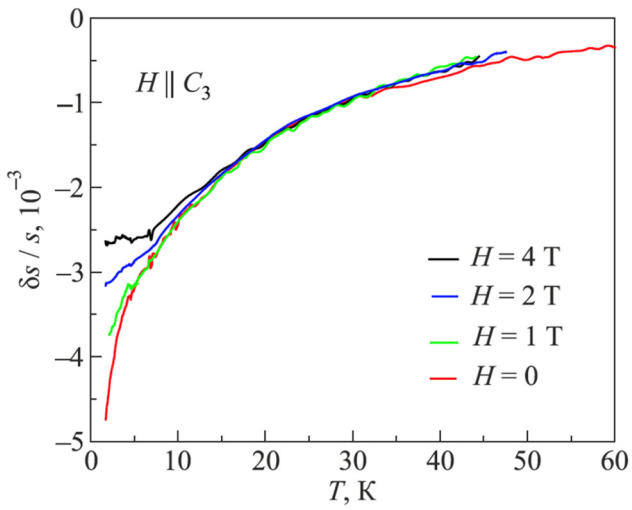

FIG. 8. The relative changes in the velocity of the C_{44}-mode as a function of temperature, under various magnetic fields. Sample No. 1.

previously noted feature, that the doublet with $i = 3, 4$ participates in the formation of temperature dependences only through the partition function.

Unlike longitudinal sound, for a transverse wave propagating along the z axis, the rotational susceptibility is nonzero and participates in the formation of its velocity. Figure 7 demonstrates the change in the velocity of the C_{44}-mode in the u_{zy} configuration. The data of several successive measurements performed on the same day are given. The sample was warmed to room temperature between these measurements. The warming and subsequent cooling procedures lasted about an hour each. Clearly, the obtained dependences indicate that the observed irreproducibility of the results pertaining to the described experiments is not associated with any slow diffusion-type processes that manifest themselves with an increase in the time interval between measurements. In the low temperature limit, the change in the C_{44} modulus, and its corresponding sound velocity, is described by an expression similar to Eq. (10), and the variability of the data is associated with the features of forming the angular coordinate φ.

Comparing the curves presented in Figs. 6 and 7, we draw attention to their obvious difference: the velocity of the C_{44}-mode at $T < 5$ K falls off noticeably faster, with a slope that increases with decreasing temperature. Even an approximate description of the velocity's behavior in this temperature range using the spectra in Table III is impossible. All that remains is to assume that, in this case, we are seeing the effects of how the populations of the smaller-scale energy structures evolve, as a result of ground doublet splitting by the Jahn–Teller and hyperfine interactions. An indirect confirmation of this assumption is the behavior of the u_{zy}-mode velocity in a magnetic field $H \| C_3$ (Fig. 8). Since its value is not too high (2–4 T), such a field does not change the average orientation of the director, nor does it complicate the modulation of its position by external deformation, so that in the high temperature range the sound velocity is practically independent of H. However, in the helium temperature range, the magnetic-field-induced transformation of the spectrum is enough for the rare-earth ion to appear in the ground, lowest energy state, where there are very few changes, and the temperature evolution of the velocity flattens out.

Although the scale of the decrease in the velocity of the C_{44}-mode is rather small, the increase in the rate of this change with decreasing temperature suggests that the system is "preparing" for some kind of phase transition. To test this assumption, measurements of the C_{44}-mode velocity were extended to a lower temperature range (1.6–0.3 K), and another sample (No. 2) was investigated. The equipment used had a somewhat different measurement algorithm,[22] and operated at higher frequencies (~100 MHz). Note that no noticeable frequency dependence was expected for the frequencies used in the described experiments. However, given the significant variability of the results noted above, the direct "stitching" of data obtained using different samples, or in different measurement cycles, is quite problematic. Figure 9 shows the velocity of the C_{44}-mode as a function of the magnetic field, recorded for samples No. 1 and No. 2 at practically the same temperatures. It can be seen that the results are very different in scale. However, it turns out that functionally, the field dependences practically coincide, within a scale factor along the ordinate axis (~0.272), which is illustrated in Fig. 9. It is assumed that the same scale factor, obtained during specific measurement cycles at a fixed temperature, will make it possible to match the temperature variations with respect to velocity that were recorded during the same cycles. Figure 10 shows a low temperature fragment of the results presented in Fig. 8, for sample No. 1, corrected by multiplying by the above-mentioned scale factor, as well as the data obtained for sample No. 2. The results of both experiments look like a single whole, and the slopes of the temperature dependences at $H = 0$ practically coincide. The latter is very important, since the

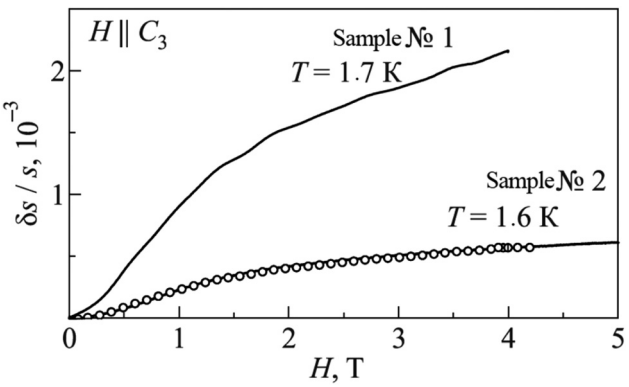

FIG. 9. The velocity of the C_{44}-mode as a function of the magnetic field. Solid lines show the experimental dependences for different samples. (○) show the dependence for sample No. 1, multiplied by a scale factor of 0.272.

procedure for estimating the scale factor from Fig. 9 does not imply a match of nonzero temperature derivatives recorded by these experiments. Therefore, it can be concluded that a temperature-independent scale factor serves as a quantitative measure of variability. In accordance with Eqs. (4) and (10), it can be identified with the $\sin^2\varphi$ parameter, which varies from experiment to experiment.

An analysis of the high-resolution optical spectra of Ho^{3+} ions[8] shows that hyperfine interaction causes each level of the ground doublet to decay into eight practically equidistant components, with $\Delta \approx 0.2$–0.3 K as distance between the lines. It could be assumed that the velocity of sound as a function of temperature

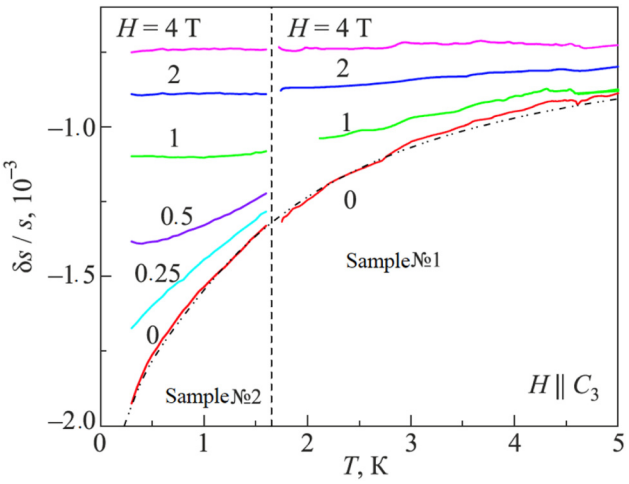

FIG. 10. Comparison of changes to the C_{44}-mode velocity, in the helium temperature range. To the left of the vertical dashed line are the results for sample No. 2, to the right are the results for sample No. 1, multiplied by a scale factor of 0.272. The dash-dot line shows the approximation (see text).

below 5 K at $H = 0$, shown on Fig. 10, is approximated by Eq. (3) using all eight lines separated by intervals of Δ,

$$\frac{\delta s}{s} \sim \frac{1}{Z}\sum_{n=0}^{7} a_n \exp(-n\Delta/T). \tag{11}$$

Since the number of phenomenological coefficients is quite large, it is possible to select them given a sufficiently good approximation of the experimental dependence for small enough Δ. An example of such a construction for $\Delta = 0.3$ K is also shown in Fig. 10. However, for a satisfactory description of the relatively noticeable temperature changes above 1–2 K, it is necessary to choose large values of parameters a_6 and a_7 that also drastically compensate each other. For example, for the approximated dependence shown in Fig. 10, these values exceed a_0 and a_1 by an order of magnitude. As already noted, the physical meaning of the coefficients in the numerators of Eqs. (3) and (11) is reduced to the "acceleration" with which the corresponding level moves along the energy scale, under the action of an external force. There are no reasons to think that the neighboring levels of the noninteracting ions' hyperfine structure subject to deformation perturbation would have significantly different motion characteristics. It is possible that the behavior of the C_{44}-mode velocity is already affected either by the manifestation of a weak exchange interaction between rare-earth ions, or by the collectivization of Jahn–Teller distortions. Neither of these effects are taken into account by Eq. (11).

In conclusion, let us condense the main results of the conducted experiments. The main elastic moduli and piezomodulus are determined by measuring the absolute velocities of sound in holmium alumoborate single crystals. The permittivity and piezoresponse renormalization, caused by the occurrence of an anisotropic nematic-like paramagnetic phase in the sample and, as a consequence, an increase in the corresponding rotational susceptibilities, has been studied. It is shown that at $T > 5$ K, the temperature dependences of the examined parameters are well-described by the ground multiplet spectrum of Ho^{3+} ions proposed in Ref. 7, formed by the interaction with a crystal field. The results are found to be significantly variable (irreproducible), which occurs, presumably, because under the influence of external fields, the motion trajectory of the nematic-like phase's director depends on random defects of thermoelastic origin. The development of uniaxial anisotropy is accompanied by a softening of all elastic moduli for which the characteristic deformations lead to angular displacements of the director. These processes are likewise characterized by the same type of variability. Softening at subkelvin temperatures is studied using the C_{44} modulus as an example. It is shown that the sound velocity as a function of temperature, which is subject to variation and obtained for different samples, can be "stitched" together using a temperature-independent scale factor, presumably determined by the director's trajectory. It is concluded that it is impossible to provide a physically consistent description of how the C_{44}-mode velocity evolves at $T < 5$ K, by averaging the magnetoelastic interaction over the hyperfine energy structure of the rare-earth ion.

ACKNOWLEDGMENTS

The authors are deeply grateful to S. V. Zherlitsyn and D. I. Gorbunov for their assistance in carrying out the low temperature measurements, and also to A. A. Zvyagin for the stimulating discussions.

REFERENCES

[1]A. I. Begunov, A. A. Demidov, I. A. Gudim, and E. V. Eremin, JETP Lett. **97**, 611 (2013).
[2]K.-C. Liang, R. P. Chaudhury, B. Lorenz, Y. Y. Sun, L. N. Bezmaternykh, V. L. Temerov, and C. W. Chu, Phys. Rev. B **83**, 180417 (2011).
[3]A. L. Freydman, A. D. Balaev, A. A. Dubrovskiy, E. V. Eremin, V. L. Temerov, and I. A. Gudim, J. Appl. Phys. **115**, 174103 (2014).
[4]A. L. Freydman, A. A. Dubrovskiy, V. L. Temerov, and I. A. Gudim, FTT **60**, 515 (2018).
[5]V. I. Zinenko, M. S. Pavlovskiy, A. S. Krylov, I. A. Gudim, E. V. Eremin, JETP, **144**, 1174 (2013).
[6]V. Kostyuchenko, V. Y. Ivanov, A. A. Mukhin, A. I. Popov, and A. K. Zvezdin, IEEE T. Magn. **50**, 1 (2014).
[7]A. I. Begunov, D. V. Volkov, and A. A. Demidov, FTT **56**, 498 (2014).
[8]A. Baraldi, R. Capelletti, M. Mazzera, N. Magnani, I. Földvári, and E. Beregi, Phys. Rev. B **76**, 165130 (2007).
[9]I. A. Gudim, E. V. Eremin, and V. L. Temerov, J. Cryst. Growth **312**, 2427 (2010).
[10]E. A. Masalitin, V. D. Fil, K. R. Zhekov, A. N. Zholobenko, T. V. Ignatova, and S. I. Lee, FNT **29**, 93 (2003) [Low Temp. Phys. **29**, 72 (2003)].
[11]T. N. Gaidamak, I. A. Gudim, G. A. Zvyagina, I. V. Bilych, N. G. Burma, K. R. Zhekov, and V. D. Fil, FNT **41**, 792 (2015) [Low Temp. Phys. 41, 614 (2015)].
[12]T. N. Gaydamak, I. A. Gudim, G. A. Zvyagina, I. V. Bilych, N. G. Burma, K. R. Zhekov, and V. D. Fil, Phys. Rev. B **92**, 214428 (2015).
[13]I. V. Bilych, K. R. Zhekov, T. N. Gaidamak, I. A. Gudim, G. A. Zvyagina, and V. D. Fil, FNT **42**, 1419 (2016) [Low Temp. Phys. **42**, 1112 (2016)].
[14]M. P. Kolodyazhnaya, G. A. Zvyagina, I. V. Bilych, K. R. Zhekov, N. G. Burma, V. D. Fil, and I. A. Gudim, FNT **44**, 1712 (2018) [Low Temp. Phys. **44**, 1341 (2018)].
[15]M. P. Kolodyazhnaya, G. A. Zvyagina, I. A. Gudim, I. V. Bilych, N. G. Burma, K. R. Zhekov, and V. D. Fil, FNT **43**, 1151 (2017) [Low Temp. Phys. **43**, 924 (2017)].
[16]V. D. Fil, M. P. Kolodyazhnaya, G. A. Zvyagina, I. V. Bilych, and K. R. Zhekov, Phys. Rev. B **96**, 180407 (2017).
[17]L. D. Landau and E. M. Lifshitz, *Theory of Elasticity* (Nauka, Moscow, 1987).
[18]M. P. Kolodyazhnaya, G. A. Zvyagina, I. V. Bilych, K. R. Zhekov, N. F. Kharchenko, and V. D. Fil, FNT **43**, 1556 (2017) [Low Temp. Phys. 43, 1240 (2017)].
[19]A. A. Demidov, N. P. Kolmakova, L. V. Takunova, and D. V. Volkov, Physica B **398**, 78 (2007).
[20]L. D. Landau and E. M. Lifshitz, *Electrodynamics of Continuous Media* (Nauka, Moscow, 1982).
[21]A. K. Zvezdin, V. M. Matveev, A. A. Mukhin, and A. I. Popov, *Rare Earth Ions in Magnetically Ordered Crystals* (Nauka, Moscow, 1985).
[22]S. Zherlitsyn, S. Yasin, J. Wosnitza, A. A. Zvyagin, A. V. Andreev, and V. Tsurkan, Fiz. Nizk. Temp. **40**, 160 (2014) [Low Temp. Phys. **40**, 123 (2014)].

Translated by AIP Author Services